

Enhanced g factors of a one-dimensional hole gas with quantized conductance

A. J. Daneshvar, C. J. B. Ford, A. R. Hamilton, M. Y. Simmons, M. Pepper, and D. A. Ritchie
Cavendish Laboratory, University of Cambridge, Madingley Road, Cambridge CB3 0HE, United Kingdom

(Received 6 February 1997)

We have measured the transport properties of quasi-one-dimensional ballistic constrictions defined on a high-mobility two-dimensional hole gas. The conductance quantization of the constrictions is changed from even to odd multiples of e^2/h as a function of the magnetic field in the plane of the heterojunction, as spin splitting causes the subbands of the one-dimensional (1D) channel to cross. We calculate the in-plane g factors of the 1D subbands using the magnetic fields at which crossing occurs and find that they increase as the number of occupied 1D subbands decreases. We attribute this enhancement of the g factor to Coulomb interactions. [S0163-1829(97)50220-7]

Hole gases provide an ideal system for the study of interaction effects in semiconductors because the hole effective mass is significantly larger than that of electrons. Thus, although the Coulomb interaction between holes is similar to that between electrons, the kinetic energy is suppressed, making interaction effects more important. Additionally, holes may be used to study band-structure effects such as mixing, nonparabolicity, and anisotropy.

Interaction effects are further enhanced in systems of reduced dimensionality. Coulomb blockade in Si-based devices¹⁻³ and lateral focusing of holes in GaAs/Al_xGa_{1-x}As heterostructures⁴ have been reported previously. However, only one paper⁵ has been published on the transport of holes through mesoscopic structures defined by gates, despite the control afforded by such devices. Reference 5 reported the observation of conductance quantization in a quasi-one-dimensional (1D) hole gas, as well as phase-coherent effects at high magnetic fields.

This work is concerned with the effect of a magnetic field on the transmission of holes through a ballistic quasi-1D constriction that connects two large regions of a two-dimensional hole gas (2DHG). We have studied the Zeeman splitting in energy of the 1D subbands by a magnetic field B applied parallel to the plane of the 2DHG but perpendicular to the current flow through the constriction. We describe the splitting ΔE of the subbands by an effective g factor^{6,7} that is defined by $\Delta E = g\mu_B B$.

In this paper, we present clear evidence of the crossing of the 1D subband edges at inplane magnetic fields lower than 3 T. In conjunction with a dc-bias technique, which allows us to determine the subband energy spacings of the constrictions, we have used the magnetic fields at which the subbands cross to calculate their g factors. We find that these increase as the number of occupied subbands in the constriction decreases and discuss this in the context of heavy-hole light-hole mixing and Coulomb interactions.

All of the measurements presented in this paper were performed on Hall bars fabricated by the surface processing of wafers grown by molecular beam epitaxy on the 311A surface of semi-insulating GaAs. The 2DHG was confined to a 200 Å wide well in a GaAs/Al_xGa_{1-x}As heterostructure ($x=0.33$), which was approximately symmetrically modulated doped using Si acceptors. The symmetry of the confin-

ing potential was confirmed by measurements of Shubnikov-de Haas oscillations, which exhibited no beating.⁸ The particular wafer used for these studies had a carrier density of $1.8 \times 10^{15} \text{ m}^{-2}$ and a very high mobility of $120 \text{ m}^2 \text{ V}^{-1} \text{ s}^{-1}$, below 1.5 K, which was found to be isotropic. The 2DHG was contacted using annealed AuBe Ohmic contacts.

The 1DHG was obtained by the application of a positive voltage to NiCr/Au Schottky split gates patterned onto the Hall bars using electron-beam lithography. A schematic diagram of device A, in which gate metal is shown shaded, is included as an inset in Fig. 1. The central gate provided extra control of the potential profile of the constriction and was held at -0.4 V for all of these experiments. We also studied

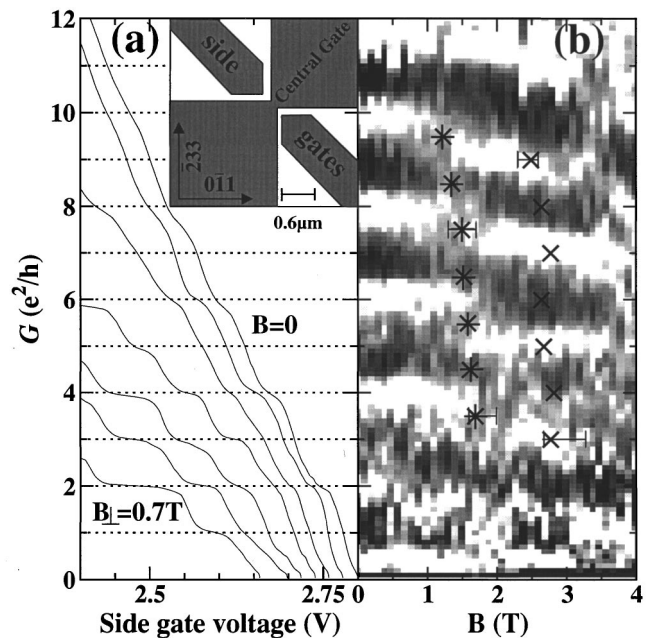


FIG. 1. (a) G vs V_g , for different B perpendicular to the 2DHG, showing good ballistic quantization at $B=0$. The inset is a schematic diagram of device A. (b) G vs B parallel to the 2DHG. The z axis is $-\partial V_g / \partial G$; white regions represent plateaus in G vs V_g . The quantization changes from even to odd integral multiples of e^2/h . The crosses and asterisks are described in the text.

two similar devices, B and C, of differing shapes, dimensions, and orientations on the crystal. The devices were measured by standard ac techniques, using an excitation voltage of $5 \mu\text{V}$ and at a lattice temperature of 70 mK.

Figure 1(a) is a plot of the conductance G of the device against side-gate voltage V_g . The plateaus, that occur at conductances quantized in multiples of $2e^2/h$, correspond to the passage through the Fermi energy of spin-degenerate 1D subbands in the constriction. The curve has been corrected for a V_g dependent series resistance, which was determined by fitting the plateaus observed at zero magnetic field to their correctly quantized values. Figure 1(a) also shows that each of the plateaus evolves into a reflected edge state with the application of a magnetic field *perpendicular* to the 2DHG, thus providing further evidence that the constriction is a 1D ballistic conductor.

The gate voltage at which the plateaus occurred was found to vary randomly by approximately 50 mV between sweeps under nominally identical experimental conditions. Despite this, every such curve contained similar features at a given conductance. Thus the device was stable in conductance but not in gate voltage. This undesirable property of the gates was common to all our devices, and we believe it to be due to problems with the fabrication technology. Reference 5 reported even more severe device noise problems.

Figure 1(b) demonstrates the effect of a *parallel* magnetic field B on the quantization of device A. The gray scale diagram was constructed from the average of the numerical differential of five G vs V_g sweeps measured for each particular B in order to obtain $-\partial V_g/\partial G$. A white pixel at (G, B) indicates that a plateau exists at a conductance of G in the pinch-off characteristic of the constriction at that particular field. The averaging served to reduce the intrinsic sample noise in the plotted data; all of the features in the averaged data are discernable in individual sweeps. Hall voltage measurements indicated that the magnetic field was at an angle of less than 0.8° to the plane.

At low magnetic fields, the white regions of Fig. 1(b) occur close to even integral multiples of e^2/h and correspond to the spin-degenerate plateaus of Fig. 1(a). As the magnetic field is increased, the conductance becomes quantized in all, and then odd, integral multiples of e^2/h . As the field is increased further, the odd quantization begins to weaken (3.5 T to 4 T). We shall argue below that this behavior is indicative of spin splitting and crossing of the 1D subband edges of the constriction. For future reference, we have marked the lightest and darkest points $(B_j, j e^2/h)$ (j is an integer) in Fig. 1(b) with crosses. They correspond to the fields at which the odd plateaus are clearest and lie between 2.5 and 3 T. We have marked with asterisks the fields at which the quantization changes from even to odd integral multiples of e^2/h . They highlight the short range of B in which G is quantized in all multiples of e^2/h .

A parallel magnetic field lifts the twofold degeneracy of the 1D subbands and leads to neighboring subbands crossing when $g\mu_B B$ equals the $B=0$ subband energy spacing. Figure 2(a) shows this schematically with a plot of the energy of the 1D subband edges (full lines, with spin depicted by arrows) against B , for a particular V_g . The Fermi level, shown as a dashed line, is curved to account for self-consistent effects, which are expected⁹ to resist changes to the electrostatics

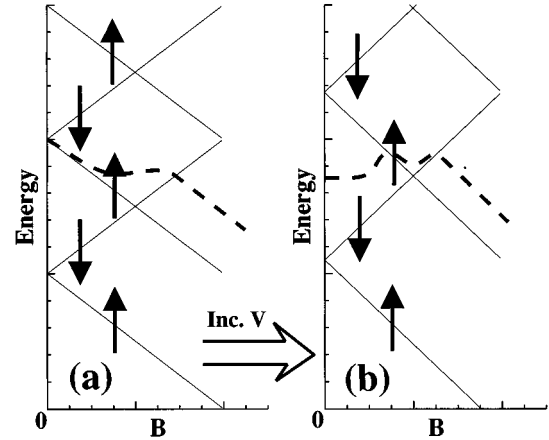


FIG. 2. (a) A schematic representation of the lifting of degeneracy of 1D subband edges by a small parallel B for a particular V_g . The Fermi level is included as a dashed line, and the arrows depict the subbands' angular momentum orientation. (b) The same as (a) but for slightly higher V_g .

(and hence carrier concentration) of the constriction by the magnetic field. Figure 2(b) indicates that an increase in V_g lowers the Fermi energy at $B=0$ and increases the subband energy spacing.

The value of the quantized conductance of the device reflects the number of 1D subbands below the Fermi energy. The applied parallel magnetic field lifts the spin degeneracy of the 1D subbands, resulting in plateaus at both even and odd integral multiples of e^2/h . A further increase in B leads to the crossing of all of the subband edges except the one lowest in energy. The conductance is now quantized in odd multiples of e^2/h . This evolution of the conductance quantization is evident in Fig. 1(b). A further increase in B causes the crossing of next-nearest 1D subbands, and the quantization is restored to even integral multiples of e^2/h .

The particularly small subband spacings in a 1DHG enable the observation of multiple crossings of subbands at fields at approximately 3 T. In principle, this behavior may be observed in electron systems too. However, the magnetic field required to cross neighboring levels is often prohibitively high, especially for the lower ones.

We have measured the energy spacings of the 1D subbands of our devices using standard dc-bias techniques.¹⁰ In Fig. 3, we plot the differential conductance $G' = \partial I/\partial V$ against source-drain dc bias V^{sd} . The gray scale uses the same averaging technique as Fig. 1(b).

The peaks in $-\partial V_g/\partial G'$ correspond to plateaus in G' vs V_g and are white in Fig. 3. The applied dc bias may change the quantization of the differential conductance to approximately odd integral multiples of e^2/h .¹¹ This occurs when, over a limited range of V_g , the number of occupied spin-degenerate 1D subbands on each side of the constriction differs by one. A further increase in the V^{sd} increases the difference to two; the quantization then reverts to even integral multiples.

The quantization of the plateaus in Fig. 3 changes from even to odd as V^{sd} is increased from zero. The white regions then drift to higher differential conductance and disappear. This increase in G' may also be observed in the highest

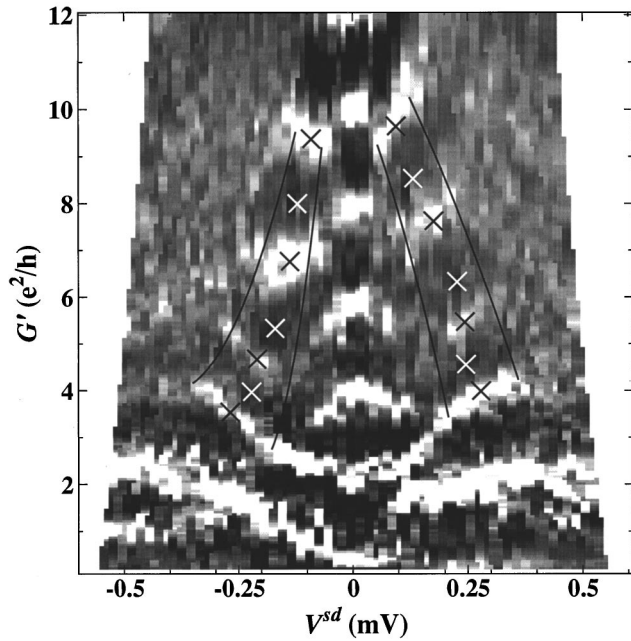


FIG. 3. Differential conductance vs dc bias (V^{sd}). The dc bias has been corrected for the series resistance of the device; the crosses are described in the text.

quality 1D electron gases,¹² and is believed to be due to nonlinear corrections to the voltage drop across the constriction. We mark the lightest and darkest points ($V_j^{sd}, je^2/h$) of Fig. 3 with crosses and indicate with solid curves generous error margins. The subband energy spacings are given by eV_j^{sd} , and increase from $90 \mu\text{eV}$ to $270 \mu\text{eV}$ as the conductance is reduced.

The g factors of each subband may be calculated by comparing the effects of the parallel magnetic field B and the electric field, due to V^{sd} , on the quantization. We assign an in-plane g factor g_j to the subbands of the constriction that are in the vicinity of the Fermi level when its conductance is quantized at je^2/h . We can determine g_j by assuming that the confining potential of the constriction at a magnetic field B_j and a source-drain bias V_j^{sd} are the same. Lifetime broadening of the quasiparticle density of states smooths the oscillation of the Fermi energy depicted in Fig. 2. We are therefore able to replace the curved Fermi energy in Fig. 2 with a horizontal line. It is assumed that the black (white) regions of Fig. 1(b), at $(B_j, je^2/h)$, correspond to the crossing (maximum spacing) of the 1D subbands. We obtain g_j by equating the Zeeman energy $g_j \mu_B B_j$ to the subband energy spacing eV_j^{sd} .

We obtain an alternative estimate of the g factors by assuming that the magnetic field at which odd and even plateaus are equally visible occurs when those subbands are equally spaced in energy. Results from device A (circles and diamonds) on two cooldowns, and device B (triangles), are presented in Fig. 4. Solid symbols represent g factors calculated using the magnetic fields at which subbands cross, and empty symbols indicate points obtained using the magnetic fields at which odd and even plateaus are equally visible. Poor data from device C are represented using arrows, which indicate lower bounds for its g factors. Our results show that g decreases from a value of over 1.3 when the constriction is

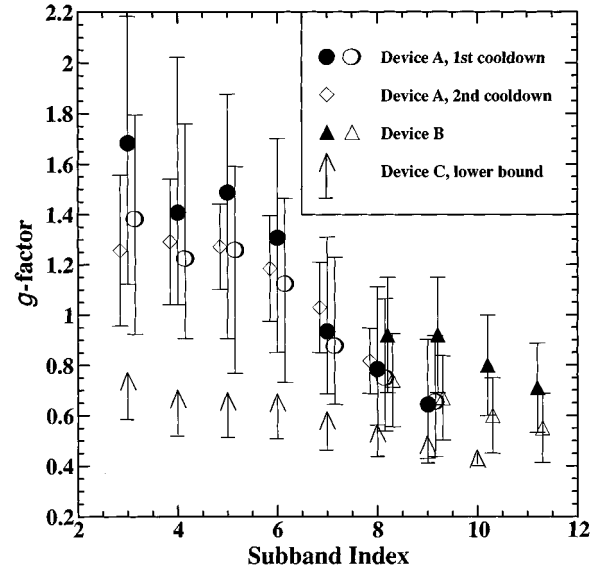


FIG. 4. The 1D subband g factors for devices A and B, calculated by comparison of, e.g., Fig. 1(b) and Fig. 3; solid symbols mark g factors calculated using the high-field set of crosses in, e.g., Fig. 1(b) while empty symbols mark g factors calculated using the low-field set. The arrows define lower bounds measured for device C.

most 1D, to ~ 0.6 when there are 11 occupied 1D subbands.

Near to the center of the Brillouin zone, the twofold degenerate 2D subbands of a symmetric quantum well are eigenstates $|M_J\rangle$ of the J_z angular-momentum operator (z is defined to be in the growth direction). They may be classified as heavy hole (HH) in which case $M_J = \pm 3/2$, or light hole (LH), for which $M_J = \pm 1/2$. In the absence of LH-HH mixing, the *in-plane* g factor of a 2D HH subband is zero,⁶ because the matrix elements $\langle \pm 3/2 | B_x J_x | \pm 3/2 \rangle$ vanish. Any reduction in the symmetry of the Hamiltonian, by the application of a lateral potential or magnetic field, or by a choice of nonzero hole wave vector, causes mixing. An increase in g then occurs because the corrections to the energies of the subbands now include nonzero matrix elements of the form $\langle \pm 1/2 | B_x J_x | \pm 3/2 \rangle$ and $\langle \pm 1/2 | B_x J_x | \pm 1/2 \rangle$.

The g factors plotted in Fig. 4 are obtained at different gate voltages, Fermi levels, and magnetic fields. Each point therefore originates from a different confining potential. In principle, the measured enhancement of the 1D in-plane g factor could be explained by increased HH-LH mixing as V_g is increased. We shall argue, however, that the resulting increase in g as the number of occupied subbands in the constriction decreases is *not* because of mixing. Instead, we suggest that the increase is due to interaction effects in the constriction.

Recent calculations¹³ of the band structure of a 2DHG confined in a symmetric quantum well similar to the one used for these experiments indicate that at our Fermi level, appreciable mixing occurs between the three lowest energy 2D subbands, which we label HH1, HH2, and LH1 in order of increasing hole energy. We believe that the lateral potential induces little *extra* mixing in the 1D subbands, because their measured energy spacings are an order of magnitude lower than the predicted gap between HH1 and HH2 (which is approximately 3 meV). Therefore our measurements have

been performed in weak lateral confinement and, in the context of mixing, the 1D subbands retain their 2D character.^{14,15} We ascribe little importance to B -field mixing because the g factors calculated from the crosses and asterisks marked at high and low fields in Fig. 1(b) are approximately consistent with one another.

When there are many occupied subbands in the constriction, the g factor is expected to be independent of the subband index with a value equal to the 2D in-plane g factor at that particular Fermi level. At our highest indices, the g factors have not yet saturated; nevertheless, we can deduce an upper limit of 0.5 for the 2D in-plane g factor.

Interactions are known to affect single-particle g factors. For example, the increase in the electron g factor with decreasing carrier concentration in Si inversion layers, and its oscillation in the quantum Hall effect, have been attributed to exchange interactions.¹⁶ Exchange effects should be of increased importance in 1D.^{17,18}

We therefore attribute our measured increase in g to Coulomb interactions, since it occurs as the carrier concentration in the constriction and the dimensionality of the interaction is reduced. A similar enhancement of the electron g factor to a value of 1.1 was recently measured.¹² This similarity be-

tween electron and hole 1D g factors, despite the differences in kinetic energy in the two systems, and in the origin of the 2D g factors, may indicate that interaction effects entirely dominate the 1D behavior. Alternatively, the reduction in HH-LH mixing due to the reduced carrier density in the constriction could lead to a reduced 2D g factor, competing with the interaction enhancement.

In conclusion, we have presented measurements of the transport properties of quasi-1D hole gases in a parallel magnetic field and have observed the spin splitting and crossing of their subbands at low B . We have measured their in-plane g factors, which begin to saturate as the system becomes quasi-2D, in the limit of high subband index. Conversely, g increases to a value of at least 1.3 in the 1D limit. We attribute this to Coulomb interactions and note that the similarity of the electron and hole 1D g factors suggests that the kinetic energy in such systems is insignificant.

We thank Roland Winkler for performing 2DHG band-structure calculations for us and Crispin Barnes for useful discussions on self-consistent effects in split gates. We also acknowledge a useful discussion with Eugene Kogan. This work was supported by the EPSRC.

¹D. J. Paul, J. R. A. Cleaver, H. Ahmed, and T. R. Whall, *Phys. Rev. B* **49**, 16 514 (1994).

²E. Leobandung, L. Guo, and S. Y. Chou, *Appl. Phys. Lett.* **67**, 2338 (1995).

³A. Yakimov, V. Markov, A. Dvurechenskii, and O. Pchelyakov, *Zh. Eksp. Teor. Fiz.* **63**, 423 (1996) [*Phys. JETP* **63**, 444 (1996)].

⁴J. J. Heremans, M. B. Santos, and M. Shayegan, *Appl. Phys. Lett.* **61**, 1652 (1992).

⁵I. Zailer *et al.*, *Phys. Rev. B* **49**, 5101 (1994).

⁶H. W. van Kesteren, E. C. Cosman, W. A. J. A. van der Poel, and C. T. B. Foxon, *Phys. Rev. B* **41**, 5283 (1990).

⁷M. J. Snelling *et al.*, *Phys. Rev. B* **45**, 3922 (1992).

⁸J. P. Eisenstein *et al.*, *Phys. Rev. Lett.* **53**, 2579 (1984).

⁹C. H. W. Barnes (private communication).

¹⁰N. K. Patel *et al.*, *Phys. Rev. B* **44**, 13 549 (1991).

¹¹L. Martin-Moreno, J. T. Nicholls, N. K. Patel, and M. Pepper, *J. Phys. Condens. Matter* **4**, 1323 (1992).

¹²K. J. Thomas *et al.*, *Phys. Rev. Lett.* **77**, 135 (1996), and private communication.

¹³R. Winkler and A. I. Nesvizhskii, *Phys. Rev. B* **53**, 9984 (1996), and private communication.

¹⁴U. Bockelmann and G. Bastard, *Phys. Rev. B* **45**, 1688 (1992).

¹⁵G. Goldoni and A. Fasolino, *Phys. Rev. B* **52**, 14 118 (1995).

¹⁶T. Ando, A. B. Fowler, and F. Stern, *Rev. Mod. Phys.* **54**, 437 (1982).

¹⁷A. Gold and A. Ghazali, *Phys. Rev. B* **41**, 8318 (1990).

¹⁸C. K. Wang and K. -F. Berggren, *Phys. Rev. B* **54**, 14 257 (1996).